

## Structural Features Amorphous-like Coatings $\text{AlN-TiB}_2\text{-TiSi}_2$ After Annealing (900, 1300) $^\circ\text{C}$ and their Impact on Physical and Mechanical Properties Changes

A.A. Demianenko<sup>1,\*</sup>, J. Partyka<sup>2</sup>, K.O. Belovol<sup>1</sup>

<sup>1</sup> Sumy State University, 2, Rymsky Korsakov Str., 40007 Sumy, Ukraine

<sup>2</sup> Lublin University of Technology, 38a, Nadbystrzycka Str., 20-618 Lublin, Poland

(Received 07 March 2014; revised manuscript received 25 May 2014; published online 29 August 2014)

The magnetron sputtered coatings on base  $\text{AlN-TiB}_2(\text{TiSi}_2)$  were investigated. The element composition, structural-phase composition, morphology were investigated before and after annealing of coatings with 900  $^\circ\text{C}$ , 1300  $^\circ\text{C}$  using SEM/EDS, AFM, SIMS, XRD, 3D Laser, Nanoindenter. The concentrations of elements in the coating were changed after annealing under 900  $^\circ\text{C}$  and further annealing under 1300  $^\circ\text{C}$ . Achieving viscoplastic index of 0.07 value when the hardness  $H = 15.3$  GPa, provides high damping properties of the coating, wherein an amorphous structure is promising to use coatings such as diffusion barriers in the form of separate elements or as a layer in contact of multilayer wear resistant coatings.

**Keywords:** Nanocomposite, Magnetron sputtering, Phase and elemental composition, Microhardness, Annealing.

PACS numbers: 61.05.cm, 61.46.Hk,  
62.20.Qp.68.37.Hk, 81.15. - z

### 1. INTRODUCTION

The structure of a film depends greatly on different factors and their reciprocal combinations. That is why investigation of phase composition, structure, physical-mechanical properties of multi-component coatings which are composed of non-metallic matrix and nanostructured metallic components based on nitrides, carbides, borides and silicides have great scientific interest [1-10].

The main aim of this work is to carry out comprehensive analysis of structure, phase composition, surface morphology of coatings which are obtained by magnetron sputtering of multicomponent target  $\text{AlN-TiB}_2\text{-TiSi}_2$  after their annealing at 900 $^\circ\text{C}$ , 1300 $^\circ\text{C}$ .

### 2. EXPERIMENTAL AND DETAILS

The high-temperature  $\text{AlN-TiB}_2$  composite with addition of  $\text{TiSi}_2$  which used as sputtered material. The coatings were annealed at 900 $^\circ\text{C}$  и 1300 $^\circ\text{C}$ .

X-ray diffraction researches of samples were performed using an X-ray diffractometer RINT-2500 V using a position-sensitive proportional counter (PSPC / MDGT). Operating voltage and current X-ray diffractometer were 40 kV and 300 mA, respectively. Measurements were made at angles of 3 $^\circ$ , 10 $^\circ$ , 30 $^\circ$ .

To study the effect of ion bombardment (ion implantation Au c 40 keV to a dose of  $10^{17}$  cm $^{-2}$ ) irradiated coating were recorded at grazing incidence angle of the smallest 2 $^\circ$  when the informative depth study of less than 100 nm.

### 3. EXPERIMENTAL AND DETAILS

An analysis of the morphology of the surface annealing at 1300 $^\circ\text{C}$  leads to a relatively low roughness of the

surface layers and the absence of explicit (as in annealing 900 $^\circ\text{C}$ ) globular substructure surface (Fig. 1).

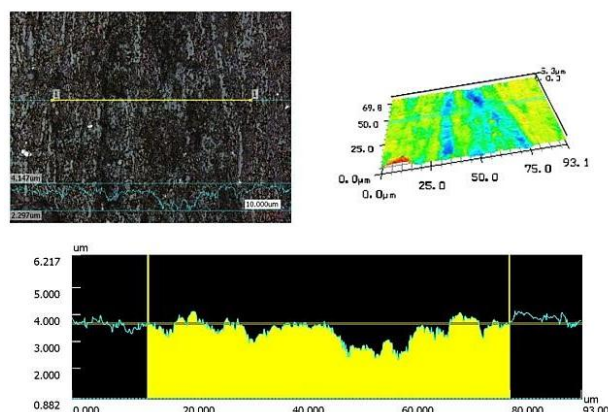


**Fig. 1** – The results of surface morphology multielement coatings  $\text{AlN-TiB}_2\text{-TiSi}_2$  after annealing at 1300 $^\circ\text{C}$  using 3D Laser + Optical method

X-ray diffraction of the samples after annealing at 900 $^\circ\text{C}$  shown in fig. 2.

Annealing leads to crystallization of the coating with a crystallite size less than 15 nm. The main phases in the crystallization -  $\text{AlN}$ ,  $\text{AlB}_2$ ,  $\text{Al}_2\text{O}_3$ ,  $\beta\text{-TiO}_2$ . Phase composition correlates of content elements in the coating, which after annealing at 900 $^\circ\text{C}$  was : B-26.49 at.%, C-6.11 at.%, N-24.32 at.%, O-10.66 a.%, Al - 20.31 at.% Si - 3.10 at.%, Ar - 1.01 at.%, Ti-8.00 at.%. Carbon, in the bound state as carbides on diffraction spectra not allocated. Thus, we can assume that determined by elemental analysis carbon is in the form of graphite nanosizes inclusions, contribution to the diffraction pattern of which is very small.

It is noted that as showed X-ray diffraction spectrum at small angles (in the sliding geometry),

\* [artem.demyanenko@gmail.com](mailto:artem.demyanenko@gmail.com)

surface layers enriched by oxide phases  $Al_2O_3$ ,  $\beta-TiO_2$  and depleted by boride by phases.

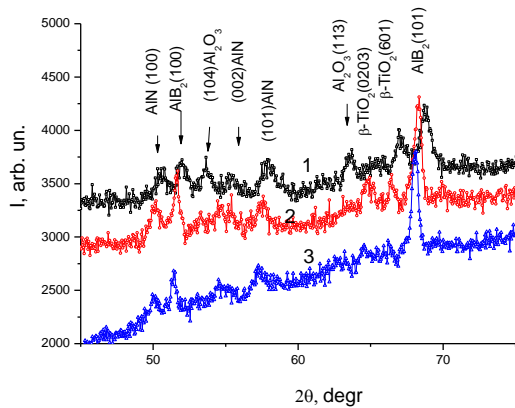


**Fig. 2** – Diffraction spectrum of  $AlN-TiB_2-TiSi_2$  coatings after annealing at  $900^\circ C$  with different scan angles: 1 -  $3^\circ$ , 2 -  $10^\circ$ , 3 -  $30^\circ$ .

On figure 3 showed the results of investigation of atomic force microscopy with a scanning area of  $10 \times 10 \mu m$  coating after annealing at  $900^\circ C$ .

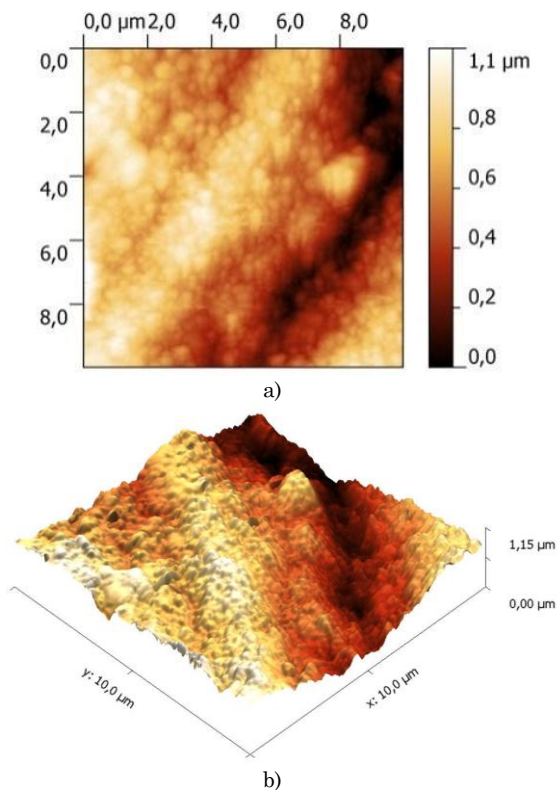


**Fig. 3** – Results of the study of atomic force microscopy with scanning area of  $10 \times 10 \mu m$  coating after annealing at  $900^\circ C$

Using the investigation method of atomic force microscopy, discovered that formed during annealing micron macrorelief has a submicron microrelief from the formation of the globule form. Comparing with the data analysis of the elemental- phase composition of the surface such forming may be as result of the formation of oxide phases on the basis of titanium and

aluminum.

On figure 4 showed diffraction spectrum of  $AlN-TiB_2-TiSi_2$  coatings after annealing  $1300^\circ C$  at different angles of scan.

It should be noted that surface depleted by boride phase as in the case of annealing at  $900^\circ C$ , and ion irradiation stimulates further depletion of the surface with boron, which appears in a relative decrease of the peaks of aluminum diboride (spectrum 4 in Fig. 4). Also to the effects of ion implantation include reduction of surface roughness coating, which results in a relatively low spread on the background of the diffraction spectrum recorded in grazing geometry.

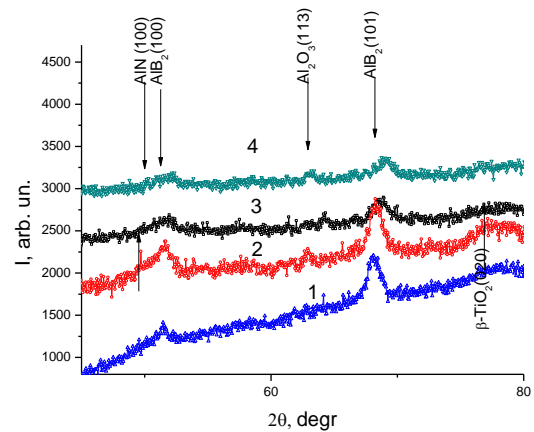


**Fig. 4** – Diffraction spectrum of  $AlN-TiB_2-TiSi_2$  coatings after annealing  $1300^\circ C$  at different angles scan: 1 -  $3^\circ$ , 2 -  $10^\circ$ , 3 -  $30^\circ$ .

Map of element distribution and profiles of elements concentrations showed on figure 5.

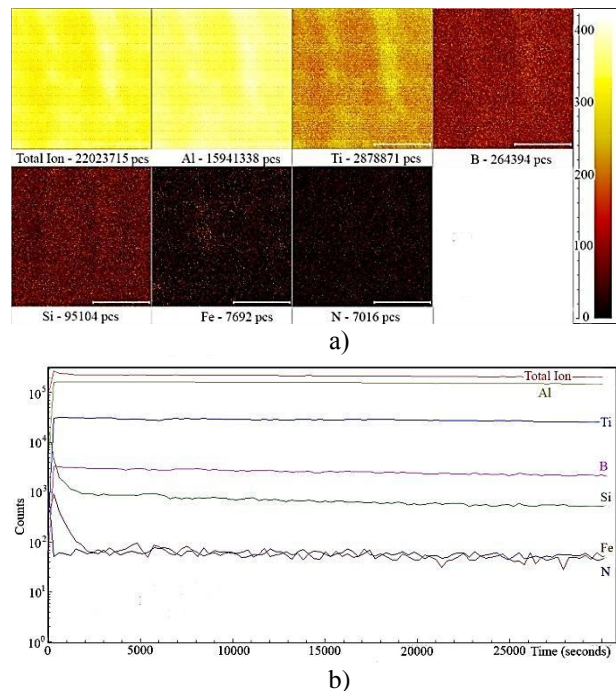


**Fig. 5** – Images of original coatings  $AlN-TiB_2-TiSi_2$ : obtained on SIMS a) Map of element distribution; b) Profiles of elements concentrations

#### 4. CONCLUSION

1. At high impact on the coating (900°C and 1300°C) observed crystallize with the formation crystallite with sizes of 11-25 nm. Annealing at the highest temperature 1300°C leads to a fundamental change in the pattern of the diffraction spectrum. The main component of the coating becomes aluminum oxide  $Al_2O_3$  and up to 30 vol.% remains of  $AlB_2$ .

2. Statistical analysis of the topography of the surface showed that the average height of the projections is 90 nm. The lateral dimensions of the

projections at the base was  $\sim 200$  nm, and the width of the projections at half height - about 70 nm.

3. It is provided high damping properties of  $AlN-TiB_2-TiSi_2$  coatings due to the obtained values of the viscoplastic index  $\approx 0.07$  with hardness  $H = 15.3$  GP which decrease after annealing of 1300°C.

4. Amorphous-like structure makes promising the using of this coatings either like diffusion barrier or like self-contained element or like contacting layer in the multilayer wear-resistant coatings.

#### REFERENCES

1. Yu.N. Tyurin, A.D. Pogrebnjak, *Surf. Coat. Tech.* **142**, 293 (2001).
2. A.D. Pogrebnjak, Yu.A. Kravchenko, S.B. Kislitsyn, Sh.M. Ruzimov, N.F. Misaelides, P.A. Hadzimitrou, *Surf. Coat. Tech.* **201**, No6, 2621 (2006).
3. A.D. Pogrebnjak, *Jour.of Nanomaterials* 780125, 1 (2013).
4. *Nanocoatings Nanosystems Nanotechnologies* (Ed. A.D. Pogrebnjak, V.M. Beresnev) (Bentham Sci.Publ. 2012).
5. A.D. Pogrebnjak, A.P. Shpak, N.A. Azarenkov, V.M. Beresnev *Phys. Usp.* **52**, 29 (2009).
6. A.D. Pogrebnjak, S. Bratushka, V.I. Boyko, I.V. Shamanin, Yu.V Tsvintarnaya, *Nucl. Instr. Meth. Phys. Res.* **145** No 3, 373 (1998).
7. D.L. Alontseva, S.N. Bratushka, A.A. Borysenko, V.N. Rogoz *Metallofiz. Nov. Tekhn.* **33** No 6, 721 (2011).
8. B.R. Zhollybekov, A.M. Mahmoud, G.V. Kirik, A.A. Dem'yanenko, *Metallofiz. Nov. Tekhn.* **35** No 6, 845 (2013).
9. A.D. Pogrebnjak, M.K. Kylyshkanov, Yu.N. Tyurin, A.Sh. Kaverina, I.V. Yakushchenko, *Techn. Phys.* **57** No 6, 840 (2012).
10. A.F. Komarov, F.F. Komarov, P. Zukowski, *Vacuum* **63** No 4, 495 (2001).
11. P. Zukowski, C. Karwat, F.F. Komarov, *phys. status solidi a* **157** No 2, 373 (1996).